

# Hox-C9 activates the intrinsic pathway of apoptosis and is associated with spontaneous regression in neuroblastoma

H Kocak<sup>1</sup>, S Ackermann<sup>1</sup>, B Hero<sup>1</sup>, Y Kahlert<sup>1</sup>, A Oberthuer<sup>1</sup>, D Juraeva<sup>2</sup>, F Roels<sup>1</sup>, J Theissen<sup>1</sup>, F Westermann<sup>3</sup>, H Deubzer<sup>4</sup>, V Ehemann<sup>5</sup>, B Brors<sup>2</sup>, M Odenthal<sup>6</sup>, F Berthold<sup>1</sup> and M Fischer<sup>\*,1</sup>

Neuroblastoma is an embryonal malignancy of the sympathetic nervous system. Spontaneous regression and differentiation of neuroblastoma is observed in a subset of patients, and has been suggested to represent delayed activation of physiologic molecular programs of fetal neuroblasts. Homeobox genes constitute an important family of transcription factors, which play a fundamental role in morphogenesis and cell differentiation during embryogenesis. In this study, we demonstrate that expression of the majority of the human *HOX* class I homeobox genes is significantly associated with clinical covariates in neuroblastoma using microarray expression data of 649 primary tumors. Moreover, a *HOX* gene expression-based classifier predicted neuroblastoma patient outcome independently of age, stage and *MYCN* amplification status. Among all *HOX* genes, *HOXC9* expression was most prominently associated with favorable prognostic markers. Most notably, elevated *HOXC9* expression was significantly associated with spontaneous regression in infant neuroblastoma. Re-expression of *HOXC9* in three neuroblastoma cell lines led to a significant reduction in cell viability, and abrogated tumor growth almost completely in neuroblastoma xenografts. Neuroblastoma growth arrest was related to the induction of programmed cell death, as indicated by an increase in the sub-G1 fraction and translocation of phosphatidylserine to the outer membrane. Programmed cell death was associated with the release of cytochrome *c* from the mitochondria into the cytosol and activation of the intrinsic cascade of caspases, indicating that *HOXC9* re-expression triggers the intrinsic apoptotic pathway. Collectively, our results show a strong prognostic impact of *HOX* gene expression in neuroblastoma, and may point towards a role of Hox-C9 in neuroblastoma spontaneous regression.

*Cell Death and Disease* (2013) 4, e586; doi:10.1038/cddis.2013.84; published online 11 April 2013

Subject Category: Cancer

Class I homeobox (Hox) transcription factors constitute an important family of developmental regulators, which play a fundamental role in morphogenesis and cell differentiation during embryogenesis.<sup>1</sup> In neural progenitors, *HOX* gene expression is controlled by retinoic acid (RA), fibroblast growth factors and wingless-type family members.<sup>2,3</sup> A deregulated expression of *HOX* genes has been observed in a number of malignancies.<sup>4–7</sup>

Neuroblastoma, an embryonal tumor of the sympathetic nervous system, originates from primordial neural crest cells, which are destined for sympathetic differentiation. This pediatric solid tumor shows remarkable variations in clinical presentations ranging from aggressive, therapy-resistant progression to spontaneous regression, which regularly occurs in infants both with localized and metastasized

disease. Furthermore, neuroblastoma cells show the potential to differentiate toward a sympathetic ganglion cell phenotype.<sup>8</sup> It has thus been suggested that the physiologic molecular program of neuroblast differentiation and growth control is disrupted in neuroblastoma.<sup>9</sup> This developmental arrest may be reversible in spontaneously regressing neuroblastoma, in which a delayed activation of naturally occurring processes of programmed cell death has been suspected.<sup>10–12</sup> According to its embryonic nature, many genes aberrantly expressed in neuroblastoma are involved in developmental processes.<sup>13,14</sup> Among others, several transcription factors involved in the development of autonomic neural crest derivatives, such as *MYCN* and *PHOX2B*, are implicated in the pathogenesis of neuroblastoma.<sup>15–18</sup> Furthermore, various *HOX* genes have been described to be aberrantly

<sup>1</sup>Children's Hospital, Department of Pediatric Oncology and Hematology and Center for Molecular Medicine Cologne (CMMC), University of Cologne, Kerpener Strasse 62, Cologne 50924, Germany; <sup>2</sup>Division of Theoretical Bioinformatics, German Cancer Research Center (DKFZ), Heidelberg 69120, Germany; <sup>3</sup>Department of Tumor Genetics, German Cancer Research Center (DKFZ), Heidelberg 69120, Germany; <sup>4</sup>Clinical Cooperation Unit Pediatric Oncology, German Cancer Research Center (DKFZ), Heidelberg 69120, Germany; <sup>5</sup>Institute of Pathology, University of Heidelberg, Heidelberg 69120, Germany and <sup>6</sup>Institute of Pathology, University Hospital of Cologne, Cologne 50924, Germany

\*Corresponding author: Dr M Fischer, Children's Hospital, Department of Pediatric Oncology and Hematology and Center for Molecular Medicine Cologne (CMMC), University of Cologne, Kerpener Strasse 62, Cologne 50924, Germany. Tel: +49 221 478 6816; Fax: +49 221 478 4689; E-mail: matthias.fischer@uk-koeln.de

**Keywords:** class I *HOX* cluster; Hox-C9; neuroblastoma; apoptosis; differentiation; spontaneous regression

**Abbreviations:** ABD, abdomen; Aberr, aberration; aCGH, array-comparative genomic hybridization; AG, adrenal glands; amp, amplification; C, chest; Dox, doxycycline; DSMZ, German Collection of Microorganisms and Cell Cultures; EFS, event-free survival; fav, favorable; GO, gene ontology; GOTM, Gene Ontology Tree Machine; Hox, homeobox; IGV, integrative genomics viewer; Loc, localization; NK, neck; norm, normal; OS, overall survival; PAM, prediction analysis for microarrays; RA, retinoic acid; SR, spontaneously regressive; SVM, support vector machine; unfav, unfavorable

Received 17.10.12; revised 14.2.13; accepted 19.2.13; Edited by G Raschella

expressed in neuroblastoma cell lines and primary tumors.<sup>19,20</sup> In a recent study, Mao *et al.*<sup>21</sup> reported that *HOXC9* expression is decreased in advanced-stage neuroblastoma and is involved in cell cycle control and the processes of neuroblastoma cell differentiation.

In this study, we aimed at determining the association of class I *HOX* gene expression patterns with prognostic markers and outcome in neuroblastoma. Because *HOXC9* was not only associated with favorable outcome but also with spontaneous regression, we investigated the functional consequences of *HOXC9* re-expression on neuroblastoma growth and programmed cell death.

## Results

**Expression of the *HOX* gene cluster is deregulated in neuroblastoma.** The expression patterns of the 39 class I *HOX* genes were analyzed in 649 neuroblastoma samples by microarrays, and the association with prognostic markers and patient outcome was determined. The expression of the majority of *HOX* genes correlated significantly with clinical covariates in neuroblastoma. Elevated expression of *HOXD* genes, particularly *HOXD3*, *HOXD8*, *HOXD9* and *HOXD10*, was predominantly associated with unfavorable prognostic markers and poor outcome (Supplementary Table S1 and Supplementary Figures S1 and S2). Similarly, we observed increased expression levels of more posterior *HOX* genes (*HOXA10*, *HOXA11*, *HOXA13*, *HOXC12* and *HOXC13*) in neuroblastomas with unfavorable characteristics (Supplementary Table S1). In contrast, elevated expression of the majority of the remaining *HOX* genes was significantly

correlated with favorable prognostic markers (Supplementary Table S1).

**Prediction of neuroblastoma outcome based on a *HOX* gene expression signature.** To assess the impact of *HOX* gene expression on neuroblastoma outcome, we developed a *HOX* gene expression-based classifier (Table 1a and Supplementary Table S2) using a training cohort of 75 neuroblastoma patients with maximal divergent outcome. In the training set, the classification accuracy was 85% as assessed by cross-validation. In a validation subset of 215 patients who matched the outcome criteria of the training set, the 33 *HOX* gene signature predicted patient outcome with an accuracy of 76% (Table 1b). In the entire validation set ( $n=574$ ), the classifier accurately discriminated patients with favorable and unfavorable outcome (favorable:  $n=265$ ; 5-year event-free survival (EFS),  $80.7 \pm 2.6\%$ ; 5-year overall survival (OS),  $96.0 \pm 1.2\%$ ; unfavorable:  $n=309$ ; 5-year EFS,  $49.5 \pm 3.0\%$ ; 5-year OS,  $67.1 \pm 2.8\%$ ; both  $P < 0.001$ ). In multivariate Cox regression models based on EFS and OS, the *HOX* classifier predicted patient outcome independently of age, stage and *MYCN* amplification status (Table 1c).

**Elevated *HOXC9* expression is associated with favorable prognostic markers, beneficial patient outcome and spontaneous regression.** Elevated *HOXC9* expression levels strongly correlated with lower stages, age < 18 months at diagnosis, lack of *MYCN* amplification, lack of 1p loss and favorable gene expression-based classification<sup>22,23</sup> (Figure 1a). Kaplan–Meier estimates were calculated by

**Table 1** Prognostic classification of neuroblastoma patients using a *HOX* gene expression-based classifier: (a) Classification performance of the *HOX* classifier in the training set; (b) Classification performance of the *HOX* classifier in 215 patients of the test set; and (c) Multivariate Cox regression models for the complete test set based on EFS and OS, considering single prognostic markers and the *HOX* classifier

Classifier	Patients (N)	Probes (N)	Accuracy (%)	Sensitivity (%)	Specificity (%)
(a)					
NB_d75_hox52_fsPAM_pred	75	52	85	58	96
(b)					
NB_d75_hox52_fsPAM_pred	215	40	76	63	90
Marker	Patients (N)	Available cases (N)	Hazard ratio	95% CI	P-value
(c)					
Model considering single prognostic markers and the <i>HOX</i> classifier based on EFS			574	547	
Age (< 18 months versus > 18 months)			2.06	1.48–2.87	< 0.001
Stages (1–3, 4S versus 4)			1.49	1.49–2.07	0.018
<i>MYCN</i> (amplified versus normal)			1.44	1.44–2.03	0.041
<i>HOX</i> classifier (favorable versus unfavorable)			2.13	1.48–3.06	< 0.001
Model considering single prognostic markers and the <i>HOX</i> classifier based on OS			574	568	
Age (< 18 months versus > 18 months)			4.44	2.61–7.53	< 0.001
Stages (1–3, 4S versus 4)			2.24	1.39–3.58	< 0.001
<i>MYCN</i> (amplified versus normal)			2.62	1.77–3.88	< 0.001
<i>HOX</i> classifier (favorable versus unfavorable)			3.1	1.67–5.76	< 0.001

Abbreviation: CI, confidence interval

using two independent neuroblastoma patient cohorts. The first cohort consisted of 244 neuroblastoma patients, which has been published previously by our group<sup>22</sup> and has been used by Mao and co-workers<sup>21</sup> for clinical analysis of *HOXC9* expression. This cohort was used to determine cutoff values of *HOXC9* expression levels by quartiles. The cutoff values were applied on an independent set of 405 neuroblastoma patients to determine clinical courses of patients with high, intermediate-high, intermediate-low and low *HOXC9* expressions. Patients with high *HOXC9* expression had a significantly better outcome with a 5-year OS of  $95 \pm 2\%$  as compared to patients with low *HOXC9* expression (5-year OS,  $56 \pm 5\%$ ; Figure 1b). Likewise, *HOXC9* expression levels strongly correlated with improved EFS (high *HOXC9* expression, 5-year EFS,  $82 \pm 4\%$  versus low *HOXC9* expression, 5-year EFS,  $37 \pm 5\%$ ; Figure 1c). In addition, multivariate Cox regression models based on EFS and OS, considering established risk markers (*MYCN* status, tumor stage and patient age at diagnosis), determined *HOXC9* expression as a significant independent prognostic marker for both EFS and OS (Table 2). We also investigated *HOXC9* expression levels

in infant neuroblastoma that had regressed without any chemotherapy, and compared these with infant stage 4 neuroblastoma. Notably, *HOXC9* transcript levels were significantly higher in neuroblastoma showing spontaneous regression (Figure 1d and Supplementary Table S3). Taken together, these results demonstrate that *HOXC9* transcript levels discriminate neuroblastoma patients with favorable and unfavorable outcome and indicate that elevated *HOXC9* expression is associated with spontaneous regression.

**Elevated *HOXC9* expression is associated with abdominal neuroblastoma.** As the expression of *HOX* genes is not only temporally but also spatially regulated during embryonic development, *HOXC9* expression were compared in neuroblastoma according to the primary tumor site. We observed significantly higher *HOXC9* expression levels in tumors with abdominal location in comparison to neuroblastomas located at the neck/chest or at adrenal glands (Figure 1e), which is in line with the embryonal expression pattern of *HOX* genes: *HOX* genes located towards the 5' end of the *HOX* cluster, such as *HOXC9*,

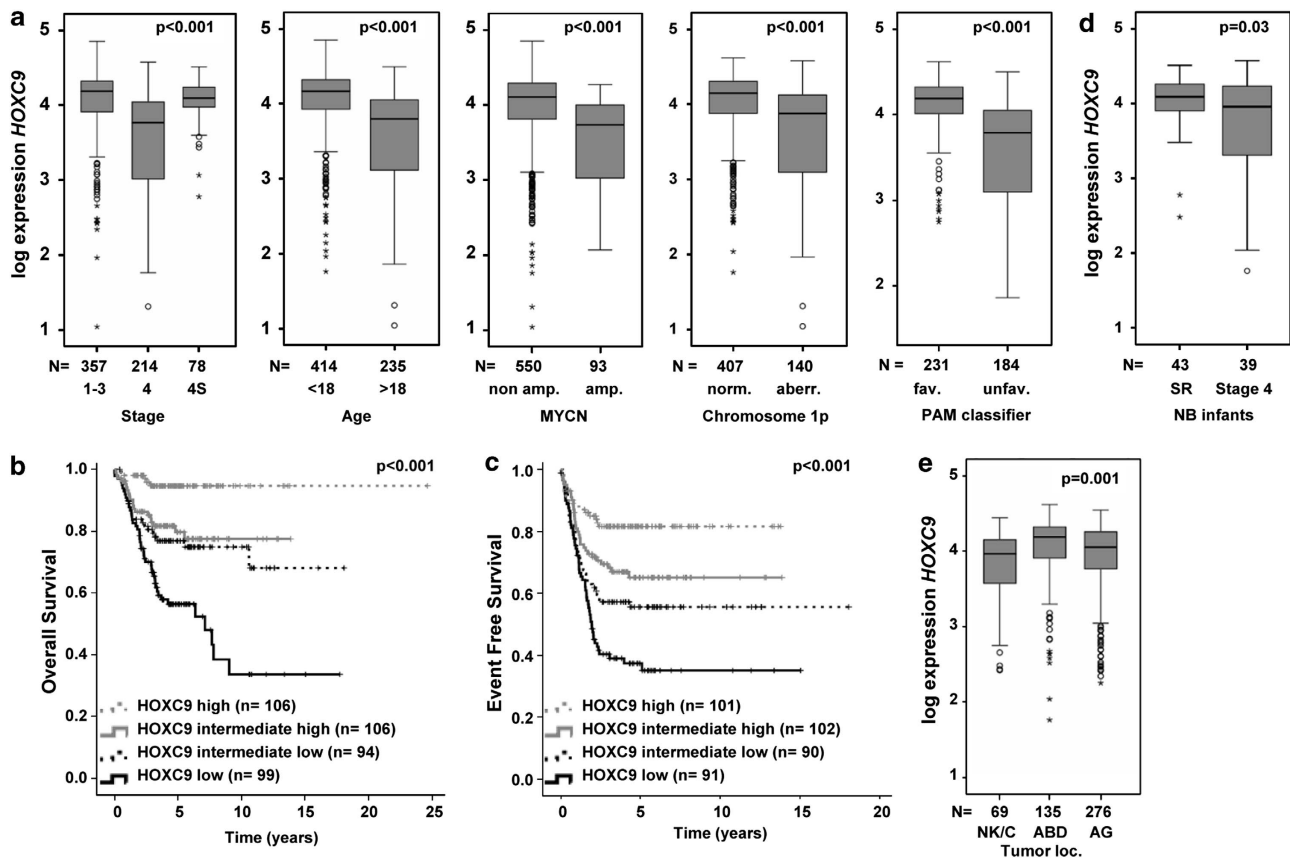


**Figure 1** (a) Association of *HOXC9* expression with prognostic markers in 649 neuroblastomas as determined by microarray analysis. PAM classifier, gene expression-based classifier as defined in the main text. Boxes, median expression values (horizontal line) and 25th and 75th percentiles; whiskers, distances from the end of the box to the largest and smallest observed values that are  $< 1.5$  box lengths from either end of the box; open circles, outlying values; asterisks, extreme outlying values. (b) OS probability in the validation set of neuroblastoma patients according to *HOXC9* expression. (c) EFS probability in the validation set of neuroblastoma patients according to *HOXC9* expression. (d) *HOXC9* expression levels in spontaneously regressing and stage 4 infant neuroblastomas. (e) *HOXC9* expression according to primary tumor localization. Amp, amplification; norm, normal; aberr, aberration; fav, favorable; unfav, unfavorable; SR, spontaneously regressive; NK, neck; C, chest; ABD, abdomen; AG, adrenal gland; Loc, localization

are expressed more posterior in the body during development. Analogous expression patterns, however, were observed for only few of the remaining 5'-located *HOX* genes (Supplementary Figure S3a). Interestingly, the spatial expression pattern of *HOXC9* might not have been expected from the association of primary tumor sites with patient outcome.<sup>24,25</sup> In line with these reports, we observed a better outcome of patients with neck/chest neuroblastoma in comparison to tumors located at the adrenal glands or in the abdomen (neck/chest versus adrenal glands versus abdomen, 5-year EFS,  $84 \pm 5\%$  versus  $69 \pm 3\%$  versus  $63 \pm 4\%$ , respectively; 5-year OS,  $97 \pm 2\%$  versus  $83 \pm 2\%$  versus  $85 \pm 3\%$ , respectively; Supplementary Figures S3b and S3c).

**Numerical gain of chromosome 12 correlates with elevated expression of *HOXC9*.** We next aimed to evaluate whether genetic or epigenetic aberrations of the *HOXC9*

locus are associated with deregulated *HOXC9* expression. First, we analyzed array-comparative genomic hybridization (aCGH) profiles of 209 neuroblastoma samples and compared the results with corresponding microarray gene expression data of the same tumors. Genomic aberrations of chromosome 12 were detected in 92/209 (44.0%) of the samples (Figure 2a and Supplementary Table S4). We most frequently observed numerical gains of the entire chromosome ( $n=64$ , 30.6%). Numerical chromosome 12 loss occurred only in four cases. Segmental alterations of chromosome 12 were detected in 24 tumors (11.5%), most of which were segmental gains not affecting the *HOXC9* locus ( $n=18$ , 8.6%). Analysis of *HOXC9* gene expression data revealed significantly higher transcript levels in tumors with numerical chromosome 12 gains in comparison to tumors in which the *HOXC9* locus was not affected by genomic alterations (Figure 2b).

**Table 2** Multivariate Cox regression models based on EFS and OS considering age at diagnosis (> 18 months versus < 18 months), stage (4 versus 1–3, 4S), *MYCN* status (amplified versus normal) and *HOXC9* expression (continuous)

Marker	Patients (N)	Available cases (N)	Hazard ratio	95% CI	P-value
<i>Model considering single prognostic markers and HOXC9 expression based on EFS</i>					
Age (> 18 months versus < 18 months)	649	622	0.48	0.34–0.66	< 0.001
Stage (4 versus 1–3, 4S)			0.52	0.38–0.72	< 0.001
<i>MYCN</i> (amplified versus normal)			0.57	0.42–0.79	0.001
<i>HOXC9</i> expression (continuous)			0.75	0.60–0.93	0.012
<i>Model considering single prognostic markers and HOXC9 expression based on OS</i>					
Age (> 18 months versus < 18 months)	649	643	0.24	0.15–0.39	< 0.001
Stage (4 versus 1–3, 4S)			0.33	0.26–0.52	< 0.001
<i>MYCN</i> (amplified versus normal)			0.32	0.22–0.46	< 0.001
<i>HOXC9</i> expression (continuous)			0.73	0.55–0.97	0.03

Abbreviations: CI, confidence interval

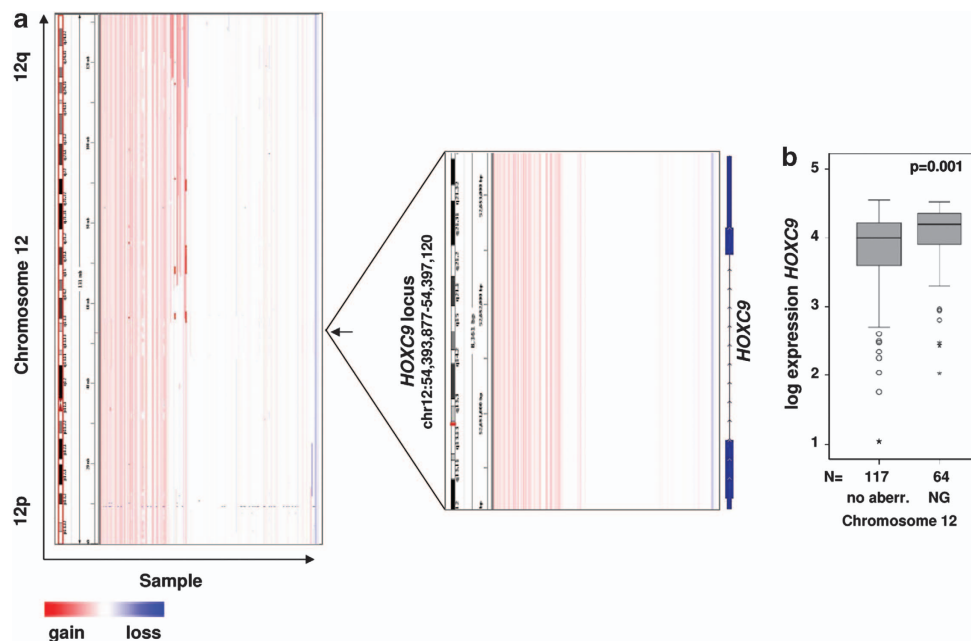


**Figure 2** Aberrations at chromosome 12 and correlation with *HOXC9* expression. (a) Chromosomal aberrations of the *HOXC9* locus in primary neuroblastomas ( $n=200$ ). (b) Association of whole chromosome 12 gain with *HOXC9* expression in primary neuroblastomas. Aberr, aberration; NG, numerical gain

To examine whether inactivating mutations might contribute to diminished *HOXC9* expression in neuroblastoma, we sequenced the genomic *HOXC9* locus of 46 primary tumors with low *HOXC9* expression. A total of 16 unique sequence variants were detected (Supplementary Table S5). Eight of these represented known SNPs, whereas the remaining sequence variants were novel. The latter variants affected either non-coding sequences or were synonymous, and occurred infrequently in our cohort. Taken together, these data suggest that mutations in the *HOXC9* locus are not a major cause of reduced *HOXC9* expression levels in unfavorable neuroblastoma.

To determine whether epigenetic regulation might contribute to differences in *HOXC9* expression in neuroblastoma, we analyzed the methylation status of 26 CpG sites located in the *HOXC9* promoter region. DNA samples from 46 neuroblastoma tumors with differing *HOXC9* expression levels (high and low *HOXC9* expression as defined in Materials and Methods,  $n = 23$  per subgroup) and 2 neuroblastoma cell lines (SK-N-AS and IMR-32) with loss of *HOXC9* expression were analyzed. Unsupervised one-way hierarchical clustering of CpG site methylation revealed a largely homogeneous methylation pattern in tumors of both subgroups and cell lines (Supplementary Figure S4b), suggesting that down-regulation of *HOXC9* does not result from altered CpG methylation patterns.

**Doxycycline-inducible expression of Hox-C9 in neuroblastoma cell lines.** *HOXC9* expression was restored in three neuroblastoma cell lines. Polyclonal Hox-C9-expressing neuroblastoma cells were compared with polyclonal GFP-expressing cells (Figure 3a) due to promoter leakage of the pRevTRE Vector System (Figure 3b). Recombinant Hox-C9 protein levels were comparable to physiological protein levels observed in neuroblastoma patients with high Hox-C9 expression (Figure 3c).

***HOXC9* expression inhibits growth of neuroblastoma cells *in vitro* and *in vivo*.** To investigate whether *HOXC9* expression affects growth properties in neuroblastoma cells, polyclonal *HOXC9*-expressing IMR-32, SK-N-AS and CHP-212 cells were compared with polyclonal *GFP*-expressing controls. Cell proliferation was assayed for up to 8 days using Trypan blue dye exclusion tests. In all cell lines, the number of viable cells at day 8 was significantly lower compared with *GFP*-induced controls (Figure 4a). To determine whether reduced proliferation upon *HOXC9* re-expression might be due to impaired cell cycle progression, the DNA content of *HOXC9*-expressing cells was assessed by flow cytometry. We observed a significant increase of the G<sub>0</sub>/G<sub>1</sub> peak at day 7 after Hox-C9 induction in all three cell lines (Figure 4b). To investigate the influence of *HOXC9* on anchorage-independent clonal growth, we performed soft agar assays. A marked reduction in colony formation was observed in both SK-N-AS and IMR-32 cells in comparison to control cells (Figure 4c). Two xenograft mouse model systems were used to assess the effect of Hox-C9 on neuroblastoma tumor growth *in vivo*. *GFP*-expressing SK-N-AS and IMR-32 control cells formed rapidly growing tumors with mean tumor volumes of  $1905 \pm 295 \text{ mm}^3$  at day 17 and  $1323 \pm 404 \text{ mm}^3$  at day 22, respectively. In contrast, tumor growth was almost completely abrogated in mice inoculated with *HOXC9*-expressing SK-N-AS and IMR-32 (tumor volumes of  $79 \pm 31 \text{ mm}^3$  at day 17 and  $173 \pm 129 \text{ mm}^3$  at day 22, respectively; Figure 4d).

**Hox-C9-induced neuronal differentiation of IMR-32 cells is accompanied by the downregulation of *REST*.** Morphological signs of neuronal differentiation were assessed by microscopic examination in all three cell lines after *HOXC9* re-expression. In IMR-32 cells, *HOXC9* re-expression led to a neuronal-like phenotype with a large network of cells interconnected by long neurite elongations (Figure 5a), while similar changes were not observed in the

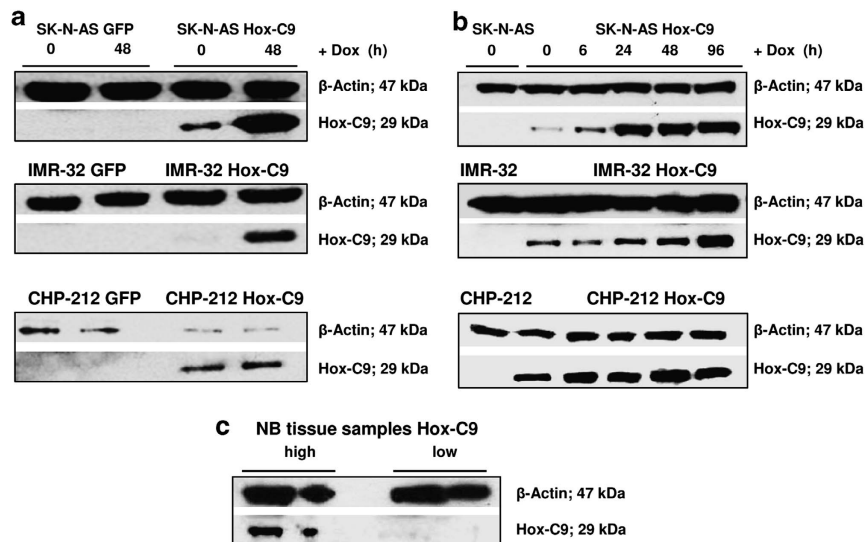


**Figure 3** Inducible expression of Hox-C9 in SK-N-AS, IMR-32 and CHP-212 cells and physiological Hox-C9 levels in primary neuroblastomas as determined by western blot analysis. (a) Inducible expression of Hox-C9- versus GFP-expressing control cells. (b) Time course of Hox-C9 expression. (c) Representative neuroblastoma tumor samples with high and low Hox-C9 expression. Dox, doxycycline; NB, neuroblastoma

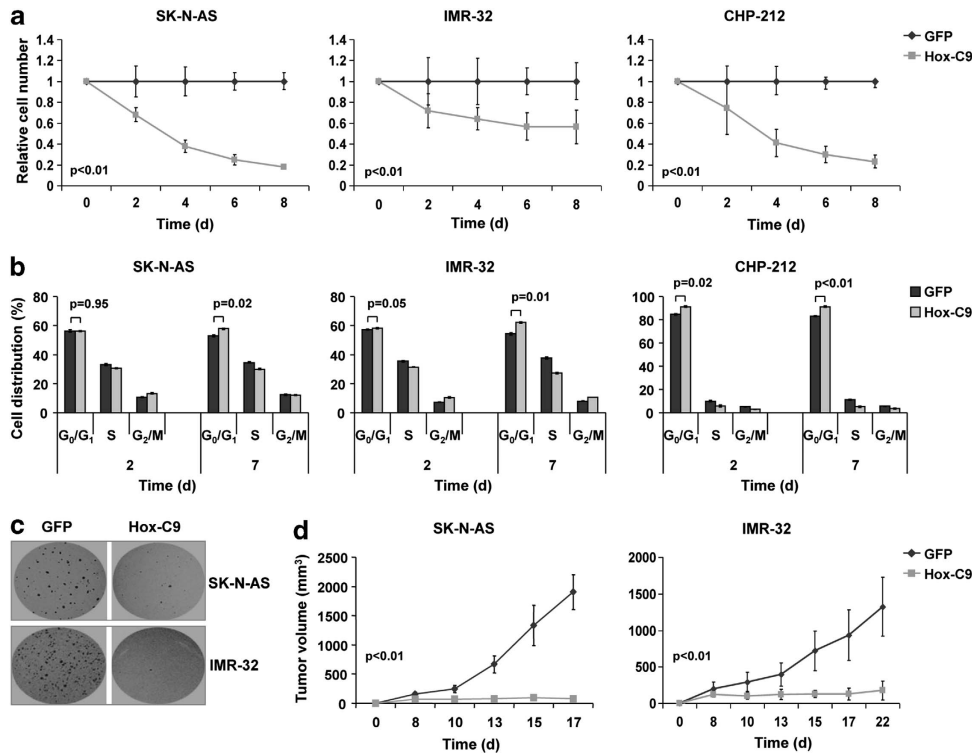


**Figure 4** *HOXC9* re-expression inhibits growth of neuroblastoma cells *in vitro* and *in vivo*. Hox-C9-induced changes in (a) cell proliferation (Trypan blue dye exclusion analysis), (b) cell cycle distribution (fluorescence-activated cell sorting (FACS)) and (c) soft agar colony formation. (d) Hox-C9 expression impede tumor growth in SK-N-AS and IMR-32 neuroblastoma xenografts ( $n = 8$  mice per group). Error bars indicate S.D.

other cell lines. To determine whether this morphological alteration induced by Hox-C9 was accompanied by the upregulation of genes involved in neuronal differentiation, we analyzed expression levels of the neuron-related markers *DNER*, *NTS*, *PTN*, *NNAT*, *TRKA* and *NEFL* by quantitative real-time reverse transcriptase-polymerase chain reactions (qRT-PCR) and microarray analysis. In line with the morphological changes, all markers were upregulated upon *HOXC9* re-expression (Figures 5b and c). A similar trend was observed for additional markers associated with neuronal differentiation (Supplementary Figure S5a and S5b). At the same time, the RE1-silencing transcription factor REST, a master negative regulator of neurogenesis, was downregulated in Hox-C9-induced IMR-32 cells (Figures 5d and e).

***HOXC9* re-expression induces apoptosis in neuroblastoma cells.** We next examined whether apoptosis contributes to the inhibition of neuroblastoma cell growth after *HOXC9* re-expression. First, externalization of phosphatidylserine was analyzed by flow cytometry using Annexin-V staining. We observed a significant increase of the Annexin-V-binding fraction in SK-N-AS and CHP-212 cells 168 h after *HOXC9* re-expression in comparison to control cells (Figure 6a). Second, DNA fragmentation was assessed using the terminal deoxynucleotidyl transferase-mediated dUTP nick-end labeling (TUNEL) assay in SK-N-AS, IMR-32 and CHP-212 cells. *HOXC9*-expressing neuroblastoma cells showed a significantly higher fraction of apoptotic cells as compared with GFP-expressing controls (Figure 6b). These results were supported by FACS analysis following Hox-C9 induction in

SK-N-AS, IMR-32 and CHP-212 cells, in which Nicoletti labeling and assessment of the fraction of sub-G<sub>1</sub> events indicated an accumulation of cells with fragmented DNA. In all investigated cell lines, the number of apoptotic cells was significantly increased by *HOXC9* re-expression as compared with GFP-induced controls (Figure 6c). Taken together, these findings indicate that Hox-C9 affects growth properties in human neuroblastoma cells not only by cell cycle regulation but also by induction of apoptosis.

**Hox-C9 activates the intrinsic pathway of apoptosis.** To further analyze Hox-C9-induced cell death, the expression of pro- and antiapoptotic regulators was examined by immunoblot, qRT-PCR and microarray analysis. Apoptotic cell death was associated with a strong increase of cytochrome *c* in the cytosolic fraction of Hox-C9-induced cells (Figure 6d), suggesting a loss of mitochondrial membrane potential and involvement of mitochondria in Hox-C9-induced cell death. In IMR-32 cells, we observed downregulation of *BCL-2* both at the transcript level and the protein level, while the expression levels remained unchanged in SK-N-AS and CHP-212 cells (Figures 6d–f). In the latter cell lines, however, we observed a marked upregulation of *BAX* mRNA expression upon induction of Hox-C9 (Figures 6e and f). These data suggest that apoptosis induced by *HOXC9* re-expression may be conferred by a shifted *BCL-2/BAX* ratio as a consequence of either increased expression of proapoptotic *BAX* or decreased expression of antiapoptotic Bcl-2. Subsequently, we investigated whether procaspase-9, the initial caspase in the mitochondrial apoptotic cascade, is activated upon

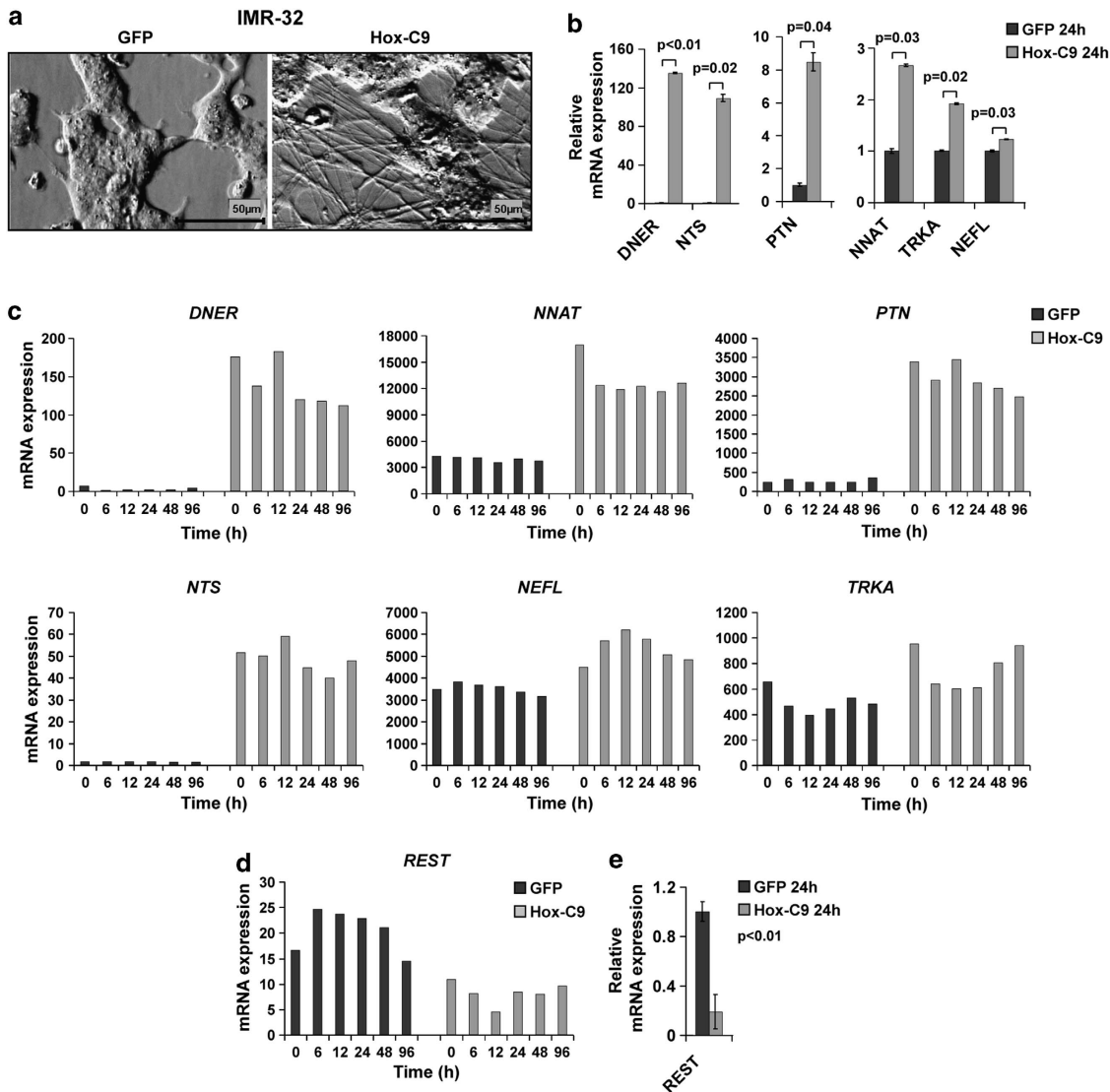


**Figure 5** Hox-C9 induces neuronal differentiation in IMR-32 cells. (a) Morphological changes of IMR-32 cells upon Hox-C9 and GFP induction at day 21. *HOXC9* expression upregulates neuron-related markers in IMR-32 cells as determined by (b) qRT-PCR and (c) oligonucleotide microarrays. Hox-C9 expression downregulates *REST* as determined by (d) oligonucleotide microarrays and (e) qRT-PCR. Error bars indicate S.D.

cytochrome *c* release. We observed an increase of cleaved 35 kDa fragments of activated caspase-9 in all cell lines upon *HOXC9* re-expression (Figure 6d). In addition, a 37 kDa cleaved fragment of caspase-9 was observed in SK-N-AS and CHP-212 cells (Figure 6d), which is indicative of a feedback amplification loop induced by activated caspase-3.<sup>26</sup> Finally, we observed an increased activation of the downstream effector caspase-3 and -7 in all three cell lines (Figure 6d) upon *HOXC9* re-expression. Taken together, these data indicate that *HOXC9* expression can activate the intrinsic pathway of apoptosis and thereby trigger neuroblastoma cell death.

**Hox-C9 affects transcriptional pathways regulating differentiation and cell death.** To gain further insights into the molecular processes occurring upon *HOXC9* re-expression, we analyzed gene expression profiles of IMR-32 and

SK-N-AS cells after Hox-C9 induction using microarrays. We used gene ontology (GO) annotations to find classes of genes that are significantly over-represented in gene sets that were either up- or downregulated after *HOXC9* re-expression (Supplementary Table S6). Many GO categories significantly enriched for genes upregulated in *HOXC9*-expressing IMR-32 cells were related to neuronal functions and differentiation, thereby reflecting the Hox-C9-associated differentiation phenotype in IMR-32 cells (Supplementary Table S6 and Supplementary Figure S7a). In SK-N-AS cells, we observed GO categories significantly enriched for genes upregulated by Hox-C9 that were associated with cell death (Supplementary Table S6 and Supplementary Figure S7c). These results are well in line with the observed phenotypes of these two neuroblastoma cell lines after *HOXC9* re-expression: While growth inhibition mediated by apoptosis is the predominant characteristic of

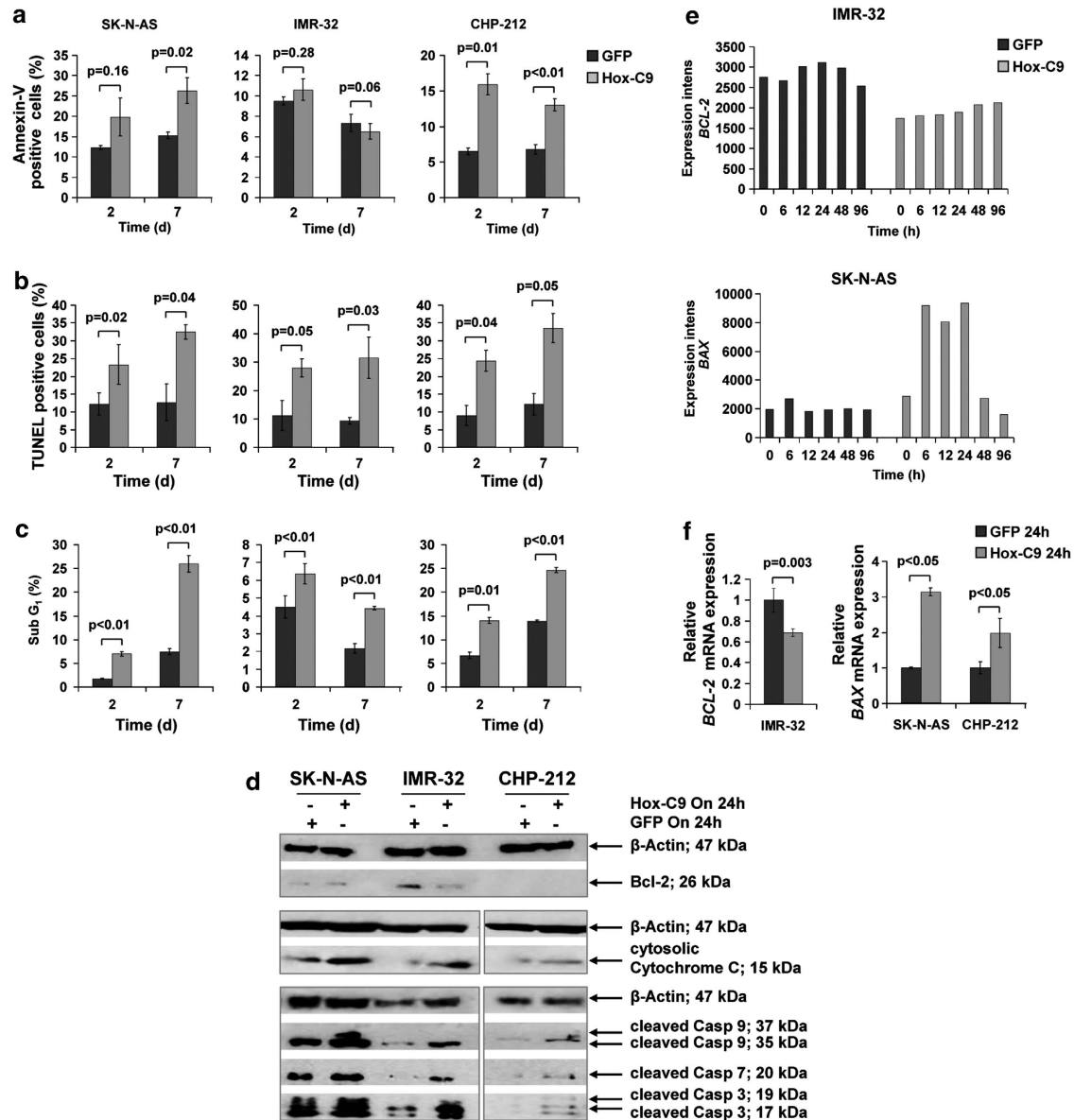


**Figure 6** Hox-C9 induces apoptosis in neuroblastoma cell lines by activating the intrinsic apoptotic pathway. (a) Proportion of Annexin-V-positive cells as determined by fluorescence-activated cell sorting (FACS). (b) Proportion of cells showing apoptotic nuclei as determined by fluorescence microscopy. (c) Proportion of cells with subnormal DNA content as determined by FACS. (d) Protein expression of Bcl-2, cytosolic cytochrome *c* and cleaved caspase-9, caspase-7 and caspase-3 upon Hox-C9 and GFP induction as determined by western blot analysis (for densitometric quantification see Supplementary Figure S6). (e) *BCL-2* and *BAX* expression in IMR-32 and SK-N-AS cells following Hox-C9 induction as determined by microarrays. (f) *BCL-2* expression in IMR-32 cells, and *BAX* expression in SK-N-AS and CHP-212 cells following Hox-C9 induction as determined by qRT-PCR. Error bars indicate S.D. Dox, doxycycline

*HOXC9*-expressing SK-N-AS cells, neuronal differentiation is mainly observed in IMR-32 cells.

## Discussion

In this study, we show that expression of the majority of class I *HOX* genes is associated with clinical phenotypes of neuroblastoma. *HOX* genes play essential roles in morphogenesis and cell differentiation during embryonic development.<sup>1</sup> As neuroblastoma is an embryonal tumor capable of differentiating into ganglioneuroma or ganglioneuroblastoma, it has been suggested that *HOX* transcription factors may be

involved in these processes.<sup>20,27</sup> Accordingly, it has been reported that morphological differentiation of neuroblastoma cells upon treatment with RA is accompanied by an increase of expression of a number of *HOX* genes.<sup>20,27,28</sup> In line with these results, we show here that the expression of most *HOX* genes is significantly associated with prognostic markers and clinical outcome in primary neuroblastoma, suggesting that *HOX* genes are essentially involved in neuroblastoma pathogenesis. The potential relevance of these genes is further emphasized by the finding that a *HOX* gene expression-based classifier was able to predict accurately neuroblastoma patient outcome independently of age, stage and

*MYCN* status. We observed that *HOX* genes of the A, B and C clusters were mainly upregulated in favorable neuroblastoma, while genes of the D cluster, particularly *HOXD3*, *HOXD8*, *HOXD9* and *HOXD10*, were upregulated in unfavorable tumors. These findings are in contrast to a recent study of Mao *et al.*,<sup>21</sup> who investigated the prognostic values of a panel of *HOX* genes in primary neuroblastoma, and did not observe any correlation of expression and clinical outcome for most of these. The difference between the two studies might be explained by the fact that Mao and co-workers<sup>21</sup> had examined a limited number of samples comprising metastasized neuroblastoma without *MYCN* amplification only,<sup>29</sup> while a large tumor cohort representing the entire spectrum of the disease has been analyzed in our study.

Among all *HOX* genes, *HOXC9* expression was most prominently associated with favorable prognostic markers and with clinical outcome. The prognostic impact of *HOXC9* is underlined by the fact that this gene was selected in all predictive models generated during the training phase of the process of *HOX* classifier generation, and that it was one of 144 genes of a prognostic classifier that we have reported previously.<sup>22</sup> Using gene expression data from our group and others, *HOXC9* expression has in addition been described to be associated with the clinical neuroblastoma phenotype in a recent study.<sup>21</sup> Notably, we observed that *HOXC9* expression levels were higher in neuroblastomas, which had spontaneously regressed than in age-related stage 4 tumors, suggesting that this transcription factor might be involved in the enigmatic molecular process of spontaneous regression.

Spatial and temporal colinearity is a hallmark of clustered *HOX* genes.<sup>30,31</sup> *HOX* genes that are positioned closer to the 5' end of the cluster, such as *HOXC9*, are expressed later and more posterior during early development. In accordance with the embryonic expression pattern of *HOX* genes, we here show a significant correlation of increased *HOXC9* expression levels of neuroblastomas from abdominal sites in comparison to tumors of the neck and chest. This finding contrasts with previous speculations,<sup>21</sup> which suggested that *HOXC9* expression might be higher in tumors of the neck and thorax because of their association with a better outcome<sup>24,25</sup> and a more differentiated histology.<sup>32</sup>

We next questioned which genetic or epigenetic factors might influence *HOXC9* expression in primary neuroblastoma. A gain of chromosome 12, which comprises the *HOXC9* locus, was associated with elevated *HOXC9* transcript levels, suggesting that a gene-dosage effect might account for *HOXC9* expression differences in neuroblastoma. These findings are in line with previous reports showing that numerical chromosomal aberrations, including chromosome 12 gain,<sup>33,34</sup> are associated with lower stages<sup>35</sup> and better outcome in neuroblastoma.<sup>36</sup> By contrast, we neither detected hypermethylation of the promoter region of *HOXC9* nor inactivating mutations in the *HOXC9* locus as a potential cause of diminished *HOXC9* expression in unfavorable tumors. Alternatively, other mechanisms, such as regulatory RNAs<sup>37</sup> or upstream transcriptional regulators,<sup>19</sup> may control *HOXC9* expression in neuroblastoma.

In line with data reported by Mao *et al.*,<sup>21</sup> we observed reduced proliferation and cell cycle arrest in the G<sub>0</sub>/G<sub>1</sub> phase upon *HOXC9* re-expression. Moreover, we substantiate that

Hox-C9 may induce neuronal differentiation in a fraction of neuroblastomas. In addition, we observed downregulation of *REST* after *HOXC9* re-expression. *REST* is a well-known master negative regulator of neurogenesis,<sup>38</sup> and has been reported to be degraded upon RA-induced neuroblastoma cell differentiation.<sup>39</sup> Taking these findings together, it seems likely that Hox-C9 promotes a more differentiated neuroblastoma phenotype by the downregulation of *REST*.

The strong effect of Hox-C9 re-expression on neuroblastoma growth arrest observed by us and others<sup>21</sup> suggested that other mechanisms than cell cycle arrest alone may contribute to this phenotype. Accordingly, we here provide substantial evidence that Hox-C9 promotes apoptosis in neuroblastoma in general, as indicated by a strong increase in the sub-G<sub>1</sub> fraction and an increase in TUNEL-positive cells after Hox-C9 induction in all three cell lines. We demonstrate that *HOXC9* expression activates the intrinsic pathway of apoptosis, probably by increasing the *BAX*:*BCL-2* ratio, which in turn leads to the release of cytochrome *c* from the mitochondria into the cytosol and activates the intrinsic cascade of caspases. Delayed activation of the naturally occurring process of programmed cell death during development of the peripheral nervous system has been suggested to represent the molecular basis of spontaneous regression in neuroblastoma.<sup>11,12</sup> Taking the correlation of *HOXC9* expression with favorable outcome and spontaneous regression in neuroblastoma, its developmental significance and its proapoptotic function in neuroblastoma cells into account, we hypothesize that Hox-C9 may contribute to the process of spontaneous regression in neuroblastoma.

In summary, we here demonstrate that distinct *HOX* gene expression patterns are associated with clinical phenotypes of neuroblastoma. We show that *HOXC9* expression does not only correlate with favorable prognostic markers and beneficial clinical outcome but also with spontaneous regression in infant neuroblastoma. Re-expression of *HOXC9* in neuroblastoma cell lines consistently leads to strong growth arrest and activates the intrinsic pathway of apoptosis. Taken together, we conclude from our data that *HOX* genes may contribute to neuroblastoma pathogenesis, and that Hox-C9 might be involved in the molecular process of spontaneous regression.

## Materials and Methods

**Patient characteristics.** Tumors of 649 neuroblastoma patients were analyzed. Stages were classified according to the International Neuroblastoma Staging System:<sup>40</sup> stage 1, *n* = 153; stage 2, *n* = 113; stage 3, *n* = 91; stage 4, *n* = 214; and stage 4S, *n* = 78. Primary tumors were localized in the abdomen (*n* = 135), at the neck/chest (*n* = 69) or the adrenal glands (*n* = 276). The primary tumor localization for the remaining 169 patients was unknown. The subgroup of patients showing regression of neuroblastoma consisted of 43 infants (localized, *n* = 14; stage 4S, *n* = 29), in which the tumor manifestations showed unambiguous regression without any cytotoxic treatment.<sup>41</sup> The neuroblastoma subgroups used for methylation and aCGH analyses consisted of 46 and 209 tumors, respectively. Risk estimation of corresponding patients was performed according to the International Neuroblastoma Risk Group (INRG) classification system<sup>42</sup> (methylation: high risk, *n* = 21; intermediate and low risk, *n* = 24; unclassified, *n* = 1; aCGH: high risk, *n* = 56; intermediate and low risk, *n* = 153).

**Gene expression analysis.** Single-color gene expression profiles from 649 neuroblastoma tumors and 2 neuroblastoma cell lines were generated using 44K

oligonucleotide microarrays as described previously.<sup>43</sup> Total RNA of *HOXC9*- and *GFP*-expressing SK-N-AS and IMR-32 cells was isolated at 0, 6, 12, 24, 48 and 96 h using Trizol (Invitrogen, Karlsruhe, Germany). To determine global differences in the expression profiles of *HOXC9*- and *GFP*-induced SK-N-AS and IMR-32 cells, mean expression levels of each gene between *HOXC9*-induced and control cells were compared. Gene Ontology Tree Machine (GOTM)<sup>44</sup> was used to identify functional categories associated with the condition of the respective cell line (Supplementary Materials and Methods). All raw and normalized microarray data are available through the Gene Expression Omnibus database (Accession: GSE45480).

**HOX gene expression-based classification.** To develop a *HOX* gene expression-based classifier (*HOX* classifier), the nearest shrunken centroids method (PAM)<sup>45</sup> was applied on *HOX* gene expression data from 75 neuroblastoma patients with maximal divergent clinical outcome.<sup>22</sup> Classification performance in the training set was evaluated by a 10 times repeated 5-fold cross-validation. Probes that were included in at least 65% of all cross-validation models were selected as classifier probes.<sup>22</sup> Classification accuracy of the final *HOX* classifier comprising 33 *HOX* genes was assessed in an independent validation set of 574 neuroblastoma patients using the support vector machine (SVM)<sup>46</sup> algorithm. Multivariate Cox proportional hazard models based on EFS and OS were used to analyze the prognostic impact of this classifier. The factors age (< 18 months versus > 18 months), tumor stage (stages 1–3 and 4S versus stage 4), *MYCN* (normal versus amplified) and *HOX* classifier were fitted into a stepwise-backward selection model.

**Analysis of genetic aberrations and promoter methylation of HOXC9.** Oligonucleotide aCGH profiles from 209 neuroblastoma tumors were generated using 44K, 105K or 1M microarrays as described previously.<sup>35,47</sup> Array-CGH analysis was performed as described previously<sup>47</sup> and visualized using the Integrative Genomics Viewer.<sup>48</sup> Because of technical reasons, 9 out of 209 aCGH profiles could not be visualized. Array-CGH data are available at Gene Expression Omnibus (Accession: GSE25771 and GSE45480). *HOXC9* promoter methylation analysis was performed by Sequenom Inc. (Hamburg, Germany; Supplementary Materials and Methods and Supplementary Table S5). Whole genome-amplified DNA from primary neuroblastoma specimens and neuroblastoma cell lines were used to sequence amplicons covering the first 500 nucleotides upstream of the *HOXC9* start site, 5'- and 3'-UTRs and the complete coding region with exon–intron boundaries. Sequencing was performed by Beckman Coulter Genomics (Danvers, MA, USA; Supplementary Materials and Methods and Supplementary Table S5).

**Data analysis and statistics.** Statistical analysis of associations between *HOX* mRNA expression levels and neuroblastoma subgroups, prognostic markers and outcome in neuroblastoma was performed using SPSS version 20.0 (IBM, Mainz, Germany). Two-tailed non-parametric tests (Mann–Whitney *U*-test and Kruskal–Wallis test) were used where appropriate. All *HOX* genes were first tested in a univariable Cox regression model based on OS and EFS. For all *HOX* genes with *P*-values ≤ 0.05, the whole cohort (*n* = 649) was divided using quartiles based on *HOX* gene expression levels. Kaplan–Meier estimates for OS (*n* = 649) and EFS (*n* = 628) were compared by log-rank test. In addition, *HOXC9* was investigated separately by using quartile values of *HOXC9* expression levels in a set of 244 neuroblastoma tumors. These values were applied on an independent set of 405 neuroblastoma expression profiles as a cutoff for high, intermediate–high, intermediate–low and low *HOXC9* expressions. Kaplan–Meier estimates for OS (*n* = 405) and EFS (*n* = 384) were compared by log-rank test. Recurrence, progression and death from disease were considered as events. Multivariate Cox proportional hazard models based on EFS and OS were used to analyze the prognostic impact of *HOXC9* expression in neuroblastoma. The factors age (> 18 months versus < 18 months), tumor stage (stage 4 versus stages 1–3 and 4S), *MYCN* (amplified versus normal) and *HOXC9* expression were fitted into a stepwise-backward selection model. The likelihood ratio test *P* for inclusion was ≤ 0.05 and for exclusion was > 0.05. Quantitative data for functional analysis were shown as means ± S.D. Unpaired two-tailed Student's *t*-tests were used where appropriate.

**Cell culture.** SK-N-AS and CHP-212 cells were obtained from ATCC (Manassas, VA, USA) and IMR-32 cells were purchased from German Collection of Microorganisms and Cell Cultures (DSMZ, Braunschweig, Germany).

Neuroblastoma cell lines were authenticated at the DSMZ. Cells were maintained as described in Supplementary Materials and Methods.

**Retroviral plasmids and stable inducible neuroblastoma cell lines.** A human *HOXC9* full open reading frame was obtained from the retroviral vector pBIG2r*HOXC9* (kind gift of Malte Buchholz, Philipps-University of Marburg, Marburg, Germany) and cloned into the pRevTRE vector (Clontech, Heidelberg, Germany; Supplementary Materials and Methods). Polyclonal neuroblastoma cell lines stably expressing either *HOXC9* or *GFP* under the control of the reverse tetracycline-controlled transactivator were generated using the RevTet System (Clontech) according to the manufacturer's instructions with marginal modifications (Supplementary Materials and Methods).

**Expression analyses using immunoblots and qRT-PCR.** Immunoblots were prepared as described previously.<sup>49</sup> Cytosolic cell extracts were isolated as described elsewhere.<sup>50</sup> Total protein extracts were isolated either with RIPA or Cell Lysis Buffer (Biovision, Hannover, Germany). Densitometric quantification of immunoblots was performed using the Image J software (NIH, Bethesda, MD, USA).<sup>51</sup> qRT-PCR was carried out two times in duplicates as described previously.<sup>52</sup> Antibody and primer information is given in Supplementary Materials and Methods and Supplementary Table S5, respectively.

**In vitro growth assays.** Cell viability was analyzed by Trypan blue dye exclusion (Supplementary Materials and Methods) and cell cycle distribution was assessed by FACS analysis as described previously.<sup>53</sup>

**Tumorigenicity assays.** Soft agar assays were used to assess the effect of *HOXC9* on colony formation ability of neuroblastoma cells (Supplementary Materials and Methods). A total of 32 six-week-old female athymic nude-Foxn1<sup>nu</sup> mice (Harlan Laboratories, Horst, The Netherlands) were used for the establishment of neuroblastoma xenograft tumors (Supplementary Materials and Methods).

**Cell viability analysis.** The TUNEL analysis was performed using the In Situ Cell Death Detection Kit according to the manufacturer's protocol (Roche, Mannheim, Germany; Supplementary Materials and Methods). Annexin-V-binding analysis was carried out using APC-coupled Annexin-V and 7-AAD according to the manufacturer's protocol (BD Biosciences, Heidelberg, Germany). Apoptotic cells were detected by FACS (FACS Canto; BD Biosciences) using the DIVA software (BD Biosciences). The extent of DNA fragmentation was evaluated in a hypodiploidy assay as described elsewhere.<sup>54</sup>

## Conflict of Interest

The authors declare no conflict of interest.

**Acknowledgements.** We thank Anne Engesser and Hafiza Fakhera Sherkheli for excellent technical assistance, Falk Hertwig for critical reading of the manuscript, Ruth Volland for statistical support and Jens Seeger for fruitful discussions. This work was supported by grants from the Cologne Center for Molecular Medicine, the Bundesministerium für Bildung und Forschung (BMBF) through the National Genome Research Network plus (NGFNplus, Grant No. 01GS0895), the Fördergesellschaft Kinderkrebs-Neuroblastom-Forschung e.V. and by the Competence Network Pediatric Oncology and Hematology (KPOH).

- Gehring WJ, Hiromi Y. Homeotic genes and the homeobox. *Annu Rev Genet* 1986; **20**: 147–173.
- Bel-Vialar S, Itasaki N, Krumlauf R. Initiating Hox gene expression: in the early chick neural tube differential sensitivity to FGF and RA signaling subdivides the HoxB genes in two distinct groups. *Development* 2002; **129**: 5103–5115.
- Nordstrom U, Maier E, Jessell TM, Edlund T. An early role for WNT signaling in specifying neural patterns of Cdx and Hox gene expression and motor neuron subtype identity. *PLoS Biol* 2006; **4**: e252.
- Daniels TR, Neacato II, Rodriguez JA, Pandha HS, Morgan R, Penichet ML. Disruption of HOX activity leads to cell death that can be enhanced by the interference of iron uptake in malignant B cells. *Leukemia* 2010; **24**: 1555–1565.
- Shears L, Plowright L, Harrington K, Pandha HS, Morgan R. Disrupting the interaction between HOX and PBX causes necrotic and apoptotic cell death in the renal cancer lines CaKi-2 and 769-P. *J Urol* 2008; **180**: 2196–2201.

6. Plowright L, Harrington KJ, Pandha HS, Morgan R. HOX transcription factors are potential therapeutic targets in non-small-cell lung cancer (targeting HOX genes in lung cancer). *Br J Cancer* 2009; **100**: 470–475.
7. Abate-Shen C. Deregulated homeobox gene expression in cancer: cause or consequence? *Nat Rev Cancer* 2002; **2**: 777–785.
8. Shimada H, Ambros IM, Dehner LP, Hata J, Joshi VV, Roald B. Terminology and morphologic criteria of neuroblastic tumors: recommendations by the International Neuroblastoma Pathology Committee. *Cancer* 1999; **86**: 349–363.
9. Nakagawara A, Arima-Nakagawara M, Scavarda NJ, Azar CG, Cantor AB, Brodeur GM. Association between high levels of expression of the TRK gene and favorable outcome in human neuroblastoma. *N Engl J Med* 1993; **328**: 847–854.
10. van Noesel MM. Neuroblastoma stage 4S: a multifocal stem-cell disease of the developing neural crest. *Lancet Oncol Mar* 2012; **13**: 229–230.
11. Pritchard J, Hickman JA. Why does stage 4s neuroblastoma regress spontaneously? *Lancet* 1994; **344**: 869–870.
12. Nakagawara A. Neural crest development and neuroblastoma: the genetic and biological link. *Prog Brain Res* 2004; **146**: 233–242.
13. Nakagawara A, Ohira M. Comprehensive genomics linking between neural development and cancer: neuroblastoma as a model. *Cancer Lett* 2004; **204**: 213–224.
14. Fischer M, Oberthuer A, Brors B, Kahler Y, Skowron M, Voith H *et al*. Differential expression of neuronal genes defines subtypes of disseminated neuroblastoma with favorable and unfavorable outcome. *Clin Cancer Res* 2006; **12**: 5118–5128.
15. Mosse YP, Laudenslager M, Khazi D, Carlisle AJ, Winter CL, Rappaport E *et al*. Germline PHOX2B mutation in hereditary neuroblastoma. *Am J Hum Genet* 2004; **75**: 727–730.
16. Pattyn A, Morin X, Cremer H, Goridis K, Brunet JF. The homeobox gene Phox2b is essential for the development of autonomic neural crest derivatives. *Nature* 1999; **399**: 366–370.
17. Schwab M, Alitalo K, Klempnauer KH, Varmus HE, Bishop JM, Gilbert F *et al*. Amplified DNA with limited homology to myc cellular oncogene is shared by human neuroblastoma cell lines and a neuroblastoma tumour. *Nature* 1983; **305**: 245–248.
18. Seeger RC, Brodeur GM, Sather H, Dalton A, Siegel SE, Wong KY *et al*. Association of multiple copies of the N-myc oncogene with rapid progression of neuroblastomas. *N Engl J Med* 1985; **313**: 1111–1116.
19. Alaminos M, Mora J, Cheung NK, Smith A, Qin J, Chen L *et al*. Genome-wide analysis of gene expression associated with MYCN in human neuroblastoma. *Cancer Res* 2003; **63**: 4538–4546.
20. Manohar CF, Furtado MR, Salwen HR, Cohn SL. Hox gene expression in differentiating human neuroblastoma cells. *Biochem Mol Biol Int* 1993; **30**: 733–741.
21. Mao L, Ding J, Zha Y, Yang L, McCarthy BA, King W *et al*. HOXC9 links cell-cycle exit and neuronal differentiation and is a prognostic marker in neuroblastoma. *Cancer Res* 2011; **71**: 4314–4324.
22. Oberthuer A, Berthold F, Warnat P, Hero B, Kahler Y, Spitz R *et al*. Customized oligonucleotide microarray gene expression-based classification of neuroblastoma patients outperforms current clinical risk stratification. *J Clin Oncol* 2006; **24**: 5070–5078.
23. Oberthuer A, Hero B, Berthold F, Juraeva D, Faldum A, Kahler Y *et al*. Prognostic impact of gene expression-based classification for neuroblastoma. *J Clin Oncol* 2010; **28**: 3506–3515.
24. Hughes M, Marsden HB, Palmer MK. Histologic patterns of neuroblastoma related to prognosis and clinical staging. *Cancer* 1974; **34**: 1706–1711.
25. Shimada H, Chatten J, Newton WA Jr., Sachs N, Hamoudi AB, Chiba T *et al*. Histopathologic prognostic factors in neuroblastic tumors: definition of subtypes of ganglioneuroblastoma and an age-linked classification of neuroblastomas. *J Natl Cancer Inst* 1984; **73**: 405–416.
26. Liu X, Kim CN, Yang J, Jemerson R, Wang X. Induction of apoptotic program in cell-free extracts: requirement for dATP and cytochrome c. *Cell* 1996; **86**: 147–157.
27. Pevaleri FA, D'Esposito M, Acampora D, Bunone G, Negri M, Faiella A *et al*. Expression of HOX homeogenes in human neuroblastoma cell culture lines. *Differentiation* 1990; **45**: 61–69.
28. Merrill RA, Ahrens JM, Kaiser ME, Federhart KS, Poon VY, Clagett-Dame M. All-trans retinoic acid-responsive genes identified in the human SH-SY5Y neuroblastoma cell line and their regulated expression in the nervous system of early embryos. *Biol Chem* 2004; **385**: 605–614.
29. Asgharzadeh S, Pique-Regi R, Sposto R, Wang H, Yang Y, Shimada H *et al*. Prognostic significance of gene expression profiles of metastatic neuroblastomas lacking MYCN gene amplification. *J Natl Cancer Inst* 2006; **98**: 1193–1203.
30. Graham A, Papalopulu N, Krumlauf R. The murine and *Drosophila* homeobox gene complexes have common features of organization and expression. *Cell* 1989; **57**: 367–378.
31. Lewis EB. A gene complex controlling segmentation in *Drosophila*. *Nature* 1978; **276**: 565–570.
32. Joshi VV, Cantor AB, Altshuler G, Larkin EW, Neill JS, Shuster JJ *et al*. Recommendations for modification of terminology of neuroblastic tumors and prognostic significance of Shimada classification. A clinicopathologic study of 213 cases from the Pediatric Oncology Group. *Cancer* 1992; **69**: 2183–2196.
33. Chen QR, Bilke S, Wei JS, Whiteford CC, Cenacchi N, Krasnoselsky AL *et al*. cDNA array-CGH profiling identifies genomic alterations specific to stage and MYCN-amplification in neuroblastoma. *BMC Genom* 2004; **5**: 70.
34. Coco S, Theissen J, Scaruffi P, Stigliani S, Moretti S, Oberthuer A *et al*. Age-dependent accumulation of genomic aberrations and deregulation of cell cycle and telomerase genes in metastatic neuroblastoma. *Int J Cancer* 2012; **131**: 1591–1600.
35. Spitz R, Oberthuer A, Zapotka M, Brors B, Hero B, Ernestus K *et al*. Oligonucleotide array-based comparative genomic hybridization (aCGH) of 90 neuroblastomas reveals aberration patterns closely associated with relapse pattern and outcome. *Genes Chromosomes Cancer* 2006; **45**: 1130–1142.
36. Janoueix-Lerosey I, Schleiermacher G, Michels E, Mosseri V, Ribeiro A, Lequin D *et al*. Overall genomic pattern is a predictor of outcome in neuroblastoma. *J Clin Oncol* 2009; **27**: 1026–1033.
37. Yekta S, Tabin CJ, Bartel DP. MicroRNAs in the Hox network: an apparent link to posterior prevalence. *Nat Rev Genet* 2008; **9**: 789–796.
38. Gao Z, Ure K, Ding P, Nashaat M, Yuan L, Ma J *et al*. The master negative regulator REST/NRSF controls adult neurogenesis by restraining the neurogenic program in quiescent stem cells. *J Neurosci* 2011; **31**: 9772–9786.
39. Singh A, Rokes C, Gireud M, Fletcher S, Baumgartner J, Fuller G *et al*. Retinoic acid induces REST degradation and neuronal differentiation by modulating the expression of SCF(beta-TRCP) in neuroblastoma cells. *Cancer* 2011; **117**: 5189–5202.
40. Brodeur GM, Pritchard J, Berthold F, Carlsen NL, Castel V, Castelberry RP *et al*. Revisions of the international criteria for neuroblastoma diagnosis, staging, and response to treatment. *J Clin Oncol* 1993; **11**: 1466–1477.
41. Hero B, Simon T, Spitz R, Ernestus K, Gnekow AK, Scheel-Walter HG *et al*. Localized infant neuroblastomas often show spontaneous regression: results of the prospective trials NB95-S and NB97. *J Clin Oncol* 2008; **26**: 1504–1510.
42. Cohn SL, Pearson AD, London WB, Monclair T, Ambros PF, Brodeur GM *et al*. The International Neuroblastoma Risk Group (INRG) classification system: an INRG Task Force report. *J Clin Oncol* 2009; **27**: 289–297.
43. Oberthuer A, Juraeva D, Li L, Kahler Y, Westermann F, Eils R *et al*. Comparison of performance of one-color and two-color gene-expression analyses in predicting clinical endpoints of neuroblastoma patients. *Pharmacogenomics J* 2010; **10**: 258–266.
44. Zhang B, Schmojer D, Kirov S, Snoddy J. GOTree Machine (GOTM): a web-based platform for interpreting sets of interesting genes using Gene Ontology hierarchies. *BMC Bioinform* 2004; **5**: 16.
45. Tibshirani R, Hastie T, Narasimhan B, Chu G. Diagnosis of multiple cancer types by shrunken centroids of gene expression. *Proc Natl Acad Sci USA* 2002; **99**: 6567–6572.
46. Vapnik VN. An overview of statistical learning theory. *IEEE Trans Neural Netw* 1999; **10**: 988–999.
47. Fischer M, Bauer T, Oberthuer A, Hero B, Theissen J, Ehrich M *et al*. Integrated genomic profiling identifies two distinct molecular subtypes with divergent outcome in neuroblastoma with loss of chromosome 11q. *Oncogene* 2009; **29**: 865–875.
48. Robinson JT, Thorvaldsdottir H, Winckler W, Guttman M, Lander ES, Getz G *et al*. Integrative genomics viewer. *Nat Biotechnol* 2011; **29**: 24–26.
49. Ackermann S, Goeser F, Schulte JH, Schramm A, Ehemann V, Hero B *et al*. Polo-like kinase 1 is a therapeutic target in high-risk neuroblastoma. *Clin Cancer Res* 2011; **17**: 731–741.
50. Kashkar H, Kronke M, Jurgensmeier JM. Defective Bax activation in Hodgkin B-cell lines confers resistance to staurosporine-induced apoptosis. *Cell Death Differ* 2002; **9**: 750–757.
51. Schneider CA, Rasband WS, Eliceiri KW. NIH Image to ImageJ: 25 years of image analysis. *Nat Methods* 2012; **9**: 671–675.
52. Fischer M, Skowron M, Berthold F. Reliable transcript quantification by real-time reverse transcriptase-polymerase chain reaction in primary neuroblastoma using normalization to averaged expression levels of the control genes HPRT1 and SDHA. *J Mol Diagn* 2005; **7**: 89–96.
53. Ehemann V, Hashemi B, Lange A, Otto HF. Flow cytometric DNA analysis and chromosomal aberrations in malignant glioblastomas. *Cancer Lett* 1999; **138**: 101–106.
54. Nicoletti I, Migliorati G, Pagliacci MC, Grignani F, Riccardi C. A rapid and simple method for measuring thymocyte apoptosis by propidium iodide staining and flow cytometry. *J Immunol Methods* 1991; **139**: 271–279.



**Cell Death and Disease** is an open-access journal published by Nature Publishing Group. This work is licensed under a Creative Commons Attribution-NonCommercial-NoDerivs 3.0 Unported License. To view a copy of this license, visit <http://creativecommons.org/licenses/by-nc-nd/3.0/>

Supplementary Information accompanies this paper on Cell Death and Disease website (<http://www.nature.com/cddis>)